Modeling System Effects and Structural Load Paths in a Wood-Framed Structure

Kenneth G. Martin[1]; Rakesh Gupta, M.ASCE[2]; David O. Prevatt, M.ASCE[3]; Peter L. Datin[4]; and John W. van de Lindt, M.ASCE[5]

Abstract: The objective of this project was to evaluate system effects and further define load paths within a light-frame wood structure under extreme wind events. The three-dimensional 30- by 40-ft (9.1- by 12.2-m) building, designed to be representative of typical light-frame wood construction in the southeastern coastal region of the United States, was modeled using SAP2000. Wall and roof sheathing was modeled using SAP's built-in thick shell element. The effect of edge nail spacing of the wall sheathing was incorporated by way of a novel correlation procedure, which eliminated the need to represent each nail individually. The computer model was validated against both two- and three-dimensional experimental studies (in plane and out of plane). Uniform uplift pressure, worst-case simulated hurricane, and ASCE 7-05 pressures were applied to the roof, and vertical foundation reactions were evaluated. The ASCE 7-05 uplift pressures were found to adequately encompass the range of uplift reactions that can be expected from a severe wind event such as a hurricane. Consequently, it was observed that ASCE 7-05 "component and cladding" pressures satisfactorily captured the building's uplift response at the foundation level without the use of "main wind force-resisting system" loads. Additionally, the manner in which the walls of the structure distribute roof-level loads to the foundation depends on the edge nailing of the wall sheathing. It was also revealed that an opening in any wall results in a loss of load-carrying capacity for the entire wall. Moreover, the wall opposite the one with the opening can also be significantly affected depending on the orientation of the trusses. In general, it was determined that complex, three-dimensional building responses can be adequately characterized using the practical and effective modeling procedures developed in this study. The same modeling process can be readily applied in industry for similar light-framed wood structures. **DOI: 10.1061/(ASCE)AE.1943-5568.0000045.**

CE Database subject headings: Residential buildings; Wind loads; Wood structures; Hurricanes.

Author keywords: Load sharing; Residential buildings; Wind loads; Wood building modeling; Hurricane loads.

Introduction

In the United States, hurricane damage to residential structures results in about $5 billion in losses annually (FEMA 2006). The vast majority of losses are the result of failure of single-family wood-framed residential structures. The most common failures in homes observed since Hurricane Camille (1969) are to roof systems, and proper anchorage (i.e., load path) is generally missing (Dikkers et al. 1970). These same concerns have repeatedly been voiced by researchers over the ensuing years, who also noted recurring widespread structural damage attributable to lack of continuity in the load paths. Poststorm reports after Hurricane Katrina revealed similar patterns of structural failures of roof sheathing loss (Fig. 1) and connection failures, as observed in Hurricane Katrina (van de Lindt et al. 2007). Arguably, improvements in hurricane resistance of residential buildings have not been sufficient in light of ample evidence from poststorm reports that concluded change is urgently needed. Wood-framed construction accounts for about 90% of the existing residential housing stock in the country, and approximately 95% of new homes. Reducing losses for residential buildings begins with forming a better understanding of the load paths from the roof to the foundation, which will likely alter the way in which light-frame wood buildings are designed for hurricane force winds.

A successful structural design, in its most basic form, must ensure that buildings are capable of supporting loads and performing their intended functions. There are two more fundamental concepts that must also be integrated into structural design, yet are often overlooked. The first concept is the need for a continuous load path. Second, designers must consider system effects that exist within the structure. Today's buildings are so complex that individual members inherently share load with their neighbors, yet these interactions are seldom incorporated into structural evaluations. This is perhaps because there is generally no practical manner by which to address system effects. It is also essential that load paths be well understood and evaluated in performing any structural analysis. Experience has shown that failure to do so leads to significant damage and even collapse (Taly 2003). History validates this notion; in the aftermath of hurricane Katrina, damage assessment teams observed widespread damage and significant patterns of structural failure attributable to a lack of load path, especially because of wind

[1]Former Graduate Research Assistant, Dept. of Wood Science & Engineering, Oregon State Univ., Corvallis, OR.

[2]Professor, Dept. of Wood Science & Engineering, Oregon State Univ., Corvallis, OR (corresponding author). E-mail: rakesh.gupta@oregonstate.edu)

[3]Assistant Professor, Dept. of Civil Engineering, Univ. of Florida, Gainesville, FL.

[4]Graduate Research Assistant, Dept. of Civil Engineering, Univ. of Florida, Gainesville, FL.

[5]Associate Professor, Dept. of Civil Engineering, Colorado State Univ., Ft. Collins, CO.

Note. This manuscript was submitted on February 25, 2010; approved on May 19, 2011; published online on November 15, 2011. Discussion period open until May 1, 2012; separate discussions must be submitted for individual papers. This paper is part of the ***Journal of Architectural Engineering***, Vol. 17, No. 4, December 1, 2011. ©ASCE, ISSN 1076-0431/2011/4-134–143/$25.00.

Fig. 1. Roof sheathing failures of houses in Hurricane Katrina (reprinted from van de Lindt et al. 2007)

uplift, as one of the prevalent failure mechanisms observed (van de Lindt et al. 2007).

Previous research has been conducted in the realm of wood-frame structures exposed to wind loads, but it has stopped short of fully addressing the mechanisms at play within these complex systems, especially in uplift scenarios. For example, much of the research has focused on specific components within the structure, such as roof or wall sheathing (Sutt 2000; Hill et al. 2009), or toward one particular type of connection, e.g., roof-to-wall (Reed et al. 1997; Riley and Sadek 2003). Very little work has addressed the system effects in full-size buildings (Asiz et al. 2010a, b). Fortunately, this shortfall can be overcome by using an analytical tool, such as a modern structural analysis computer program, which directly incorporates system effects, mainly load sharing among trusses in the roof and studs in walls.

The following tasks represent the overall objectives of this study. Throughout this research, one goal at the forefront of each task was to address very complex structural behaviors using the most pragmatic modeling techniques possible. In this manner, the authors hope to develop a practical analysis approach for use by wood engineers and designers to readily and accurately predict the behavior of similar wood structures. Specific goals were: (1) to develop a practical three-dimensional (3D) computer model of a full-size light-frame wood structure, (2) to develop a practical representation of the sheathing nailing schedule to be incorporated into the computer model, and (3) to evaluate critical load paths and system effects for different building geometries under various wind loading scenarios.

Literature Review

Mtenga (1991) developed a two-dimensional (2D) truss model with semirigid, nonlinear connections at all the joints. Although his model proved to be an accurate predictor of member forces and moments when compared with experimental results, Mtenga concluded that the model might be unnecessarily complicated. Several researchers have successfully used simplified connection (pin and rigid) models (Li et al. 1998; Gupta et al. 2004; Gupta and Limkatanyoo 2008) to successfully predict the behavior of 3D roof truss assemblies.

Many previous studies have used beam elements to model the behavior of sheathing. For example, Li et al. (1998) used three beam elements per side in their nine-truss roof assembly model to represent the roof sheathing. Their model was found to be in good agreement with experimental results. Gupta et al. (2004) and Gupta and Limkatanyoo (2008) also used frame elements in a similar fashion to simulate roof sheathing. Some researchers have explored the use of area or shell elements built in to modern structural analysis programs such as SAP. Doudak (2005) represented oriented strand board (OSB) wall sheathing in 2D shear wall tests using the shell element with elastic orthotropic material properties. Doudak fastened the sheathing to the framing members using nonlinear link elements, which exhibited strength degradation as the connection approached failure. This modeling procedure required individual link elements to model every fastener in the shear wall. Although accurate, such "meticulous detailing"—as Doudak noted—can be quite laborious to implement. Results from the analytical model were compared with similar full-scale tests, and it was found that the two were in good agreement.

Zisis (2006) also made use of SAP's shell element to model the sheathing while investigating wind effects on a low-rise wooden building. In his study, Zisis chose to represent the in-plane forces using shell membrane behavior, but excluded plate (out-of-plane bending) behavior of the element. As a result, the sheathing response in this research was limited to in-plane behavior. In addition, isotropic material properties were assigned to the membrane, which may not necessarily capture the orthotropic nature of plywood and OSB sheathing. Finally, Zisis noted that a linear model was used; however, no additional details were provided. Thus, by eliminating the nonlinear link element of Doudak's effort, it is unclear how Zisis modeled the sheathing nail connection between the shell element and the framing members. In the most recent papers, Asiz et al. (2010a, b) address issues associated with system-level modeling of timber light-frame building superstructures in elastic and overload response regimes.

The Forest Products Laboratory, based in Madison, Wisconsin, has pioneered several full-scale load sharing studies in the past 30 years. McCutcheon (1977) showed that there is an interaction between the sheathing and the joists, which tends to increase the stiffness of the floor system as a whole, but the two components do not act as if they were rigidly connected together. Wolfe and McCarthy (1989) then investigated load sharing within an assembly of roof trusses and found that stiffer trusses carry a greater share of the load, and truss deflections were far less in the assembly than outside assembly. Wolfe and LaBissoniere (1991) showed that 40–70% of the load applied to an individual truss is distributed to adjacent unloaded trusses by the plywood sheathing.

Additional load sharing and system interaction studies were also conducted by LaFave and Itani (1992), Percival and Comus (1980), and many others. A detailed literature review of these studies is presented by Gupta (2005) and is, therefore, not included in this paper.

Materials and Methods

In this study, an analytical model of a light-frame wood structure was developed and validated. The major thrust of this research has focused on the development of simple, yet accurate material

J. Archit. Eng., 2011, 17(4): 134-143

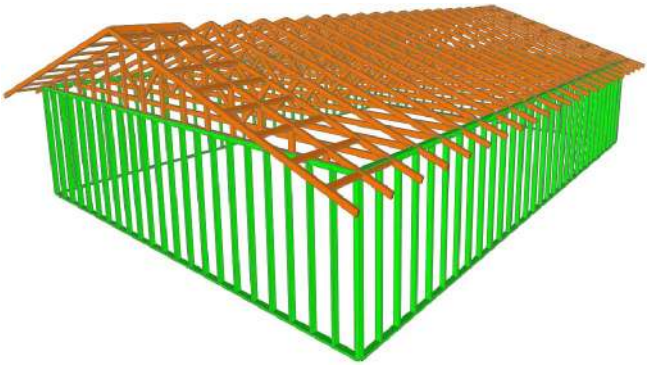

Fig. 2. SAP model of the index building (exterior sheathing not shown for clarity)

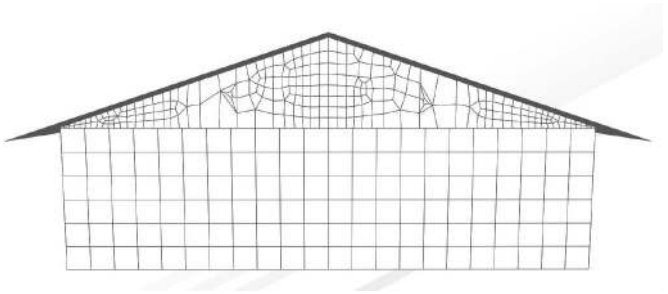

Fig. 3. Meshing of the wall sheathing in the gable ends; "general divide" was used for the triangular region above the top plate of the wall

assignments and property correlations for use in three-dimensional wood structures. Considerable efforts were made to use built-in features of the software in conjunction with simple modeling techniques to capture complex structural responses (e.g., system effects, effect of nailing schedule).

A uniform uplift pressure was applied to the roof sheathing to better understand how the model behaved under uplift loads. Several scenarios (e.g., changing anchor bolt spacing, adding an opening to one wall, increasing the building length) were considered while the structure was subjected to this uniform uplift pressure. Next, the reaction profile of the structure was compared when subjected to simulated hurricane wind uplift loads against profile subjected to ASCE 7-05 (ASCE 2005) design wind pressures.

The analytical model of the index building (Fig. 2) was developed using SAP2000 (Computers and Structures 2008). The model is composed entirely of pinned or rigid connections, and all materials are assumed to behave within the elastic range. Although some parts of the building may go in to inelastic range, the general behavior of the building most likely would be the same as in the elastic rage.

Studs and truss members are represented using frame elements with isotropic material properties. Wall and roof sheathing are modeled using the thick shell element with orthotropic material properties. Anchorage devices are represented by grounded springs.

The footprint of the index building is 29 ft, 4 in. (9 m) wide by 40 ft (12.2 m) long with overhangs on all sides. The gable roof has a 4:12 slope. Studs are spaced 16 in. (406 mm) on center, and trusses are 24 in. (610 mm) on center. The bottom plate is anchored to the foundation using 1/2-in. (12.7-mm) diameter anchor bolts spaced at 4-ft (1.2-m) intervals. At each corner of the building, there is a Simpson Strong-Tie HDU2 hold-down attached to the double stud. The roof sheathing is 1/2-in. plywood, and the wall sheathing is 7/16-in. (11 mm) OSB. There are no interior partitions (Fig. 2). Specific construction features and detailed framing plans of the index building can be found in Martin (2010).

Modeling

Shell Element Behavior

The roof sheathing [1/2-in. (12.7-mm) plywood] and wall sheathing [7/16-in. (11-mm) OSB] were modeled using SAP's thick shell element to include system effects. In the modeling environment—where the walls and roof structure are defined and manipulated—individual shell elements were used to represent each wall/roof section. That is, an individual 4×8-ft (1.2×2.4-m) sheet of plywood/OSB was not modeled, but instead an entire side wall (or roof surface) is represented by a single one shell element in SAP. SAP then automatically subdivides each modeling shell element into multiple analysis shell elements, in a process known as meshing. The user controls how the mesh is defined and can inspect the meshed "analysis model" of each shell element created (Fig. 3). The shell-element approach was verified using test results from literature as describe subsequently in the paper.

This modeling approach implicitly assumes that internal forces are transferred continuously across the joints between the actual 4×8-ft (1.2×2.4-m) sheathing panels. This practical assumption can be judged by examining the wall and roof systems in greater detail. In wall systems, blocking along all panel edges and high nailing density contribute to the validity of the assumption. In roof systems, the assumption of continuity across the joints is drawn from four sources: (1) staggered joints along truss lines, (2) edge nail spacing of 6 in. (152 mm) or less along truss lines, (3) unblocked panel edges with nails within 3/8 in. (10 mm) from the edge where trusses support the panels, and (4) "H-clips" located in the bays between trusses. Martin (2010) provides further details and accompanying figures related to this discussion.

Connectivity

The members within the truss are connected using a mixture of pinned and rigid connections. This configuration was used successfully in the research effort conducted by Gupta and Limkatanyoo (2008). The joint representing the heel of the truss is not coincident with the connection to the top plate of the wall. Since the analog of the wall members is drawn through the centerlines, these two joints are offset by a distance of 1.75 in. (44 mm) [i.e., half the width of the nominal 2×4-in. (51×102-mm) top plate]. Both of these connections (heel joint and truss to top plate) were rigid. Vertical web members in the gable end trusses and overhang framing members were considered to be pinned at each end.

All members in the walls are pinned, including stud-to-plate connections (at both ends) as well as plate-to-plate connections at the corners of the building. In this configuration, the wall framing provides no lateral stiffness unless sheathing is present.

Stiffness of Hold-Downs and Anchor Bolts

Foundation hold-down devices at the corners and anchor bolts [spaced 4 ft (1.2 m) on center] were used to fasten the external walls to the foundation. The axial stiffness of the selected hold-down device, the HDU2 (Simpson Strong-Tie 2008), is 35,000 lb/in (6,125 N/mm), which takes into account fastener slip, hold-down elongation, and bolt elongation. The axial stiffness of the anchor bolts was determined using Seaders et al. (2009) study. The shear stiffness of the anchor bolts in the X and Y-direction was determined using a procedure recommended by the American Wood Council [American Forest and Paper Association (AF&PA) 2007]. Table 1 summarizes the spring stiffness values used in this study. Additional details relating to the derivation of these values are given in Martin (2010).

J. Archit. Eng., 2011, 17(4): 134-143

Table 1. Spring Stiffness Used to Model the Anchor Bolts and Hold-Downs

Item	*X*-direction shear, lb/in. (N/mm)	*Y*-direction shear, lb/in. (N/mm)	*Z*-direction axial, lb/in. (N/mm)	Source
Hold-downs	—	—	35,000 (6,125)	Simpson Strong-Tie (2008)
Anchor bolts	65,000 (11,375)	65,000 (11,375)	35,000 (6,125)	AF&PA (2005) and Seaders (2004)

Material Properties

All framing members were nominal 2×4-in. (51×102-mm) lumber. Frame elements, which represent the wall and truss members, were modeled using elastic, isotropic material properties. At each of the four corners, three studs were nailed together and modeled as one frame element with an equivalent moment of inertia. Framing around the opening (e.g., door) had a nominal 2×12-in.(51×305-mm) header beam and double studs at both ends. The National (NDS) code (AF&PA 2005a) and the Wood Handbook (USDA 1999) were used to assign values. Additional details are provided in Martin (2010).

Wall and roof sheathing were each modeled using SAP's thick shell element. Orthotropic, elastic material properties (Tables 2 and 3) were then assigned. Nine constants are needed to describe the behavior of these materials, although only the values shown in bold (Table 3) affect the response of the model. The values given in Tables 2 and 3 were used for all wall and roof sections in the index building with one exception: the shear modulus, G_{12}, of the wall sheathing that was modified using a correlation procedure described in Martin (2010). Table 4 provides the correlated shear modulus values for the wall sheathing.

Research Methods

Verification/Validation

The following studies from literature were used to validate the model: (1) two-dimensional individual truss behavior (Wolfe et al. 1986); (2) three-dimensional roof assembly behavior (Wolfe and McCarthy 1989); (3) two-dimensional shear wall behavior (Langlois et al. 2004; Lebeda et al. 2005; Sinha and Gupta 2009); (4) three-dimensional influence functions of the entire building (Datin and Prevatt 2007). The geometry modifications listed were explored for the uniform uplift pressure load case only. Further information pertaining to each scenario is provided in Martin (2010).

Load Cases

The following load cases were explored in support of this research effort. Further information pertaining to each scenario is provided in Martin (2010).

1. Uniform uplift pressure [50 psf (2.4 kPa)];
2. Simulated hurricane uplift pressures:
   a. Load case 1—Absolute maximum uplift [90 psf (4.3 kPa)] at the corner of the roof;
   b. Load case 2—Local maxima over entire roof [10–90 psf (0.5–4.3 kPa)];
   c. Load case 3—Absolute maximum uplift [90 psf (4.3 kPa)] at the ridge of the roof;
3. ASCE 7-05 component and cladding (C&C) design pressures:
   a. Uplift acting alone [28–95 psf (1.3–4.6 kPa)];
   b. Lateral forces acting alone [32–38 psf (1.5–1.8 kPa)];
   c. Combination of uplift [28–95 psf (1.3–4.6 kPa)] and lateral forces [32–38 psf (1.5–1.8 kPa)].

Geometry Scenarios

The following geometry variations were explored for the first load case noted in the preceding section (uniform uplift pressure): (1) standard building (control case); (2) changing the edge nailing of the wall sheathing; (3) adding length to the building; (4) presence

Table 2. Elastic Isotropic Material Properties Used in the SAP Model

Item	Description	Modulus of elasticity, 10^6 psi (GPa)		Poisson's ratio	
		Value	Source	Value	Source
Wall members	Spruce-pine-fir, stud grade	1.2 (8.3)	NDS (AF&PA 2005a)	0.40	Wood Handbook (USDA 1999)
Truss members	Southern yellow pine, No.3 and stud	1.4 (9.7)		0.36	

Table 3. Elastic Orthotropic Material Properties Used in the SAP Model

Description		Modulus of elasticity (10^5 psi)			Shear modulus (10^5 psi)			Poisson's ratio[d]		
Item	Type	E_1	E_2	E_3	G_{12}	G_{13}	G_{23}	μ_{12}	μ_{13}	μ_{23}
Wall sheathing[a,b]	7/16 in. (11 mm) OSB	**7.4**	**2.3**	2.3	**1.2**	1.2	1.2	**0.08**	0.08	0.08
Roof sheathing[c]	1/2 in. (13 mm) plywood	**19**	**2.9**	2.9	**1.5**	1.5	1.5	**0.08**	0.08	0.08

[a]Modulus of elasticity and shear modulus values from Doudak (2005).
[b]Shear modulus values subject to the correlation procedure (Table 4).
[c]Modulus of elasticity and shear modulus values from Wolfe and McCarthy (1989) and Kasal (1992).
[d]Poisson's ratio from Kasal (1992).

Table 4. Correlation between Nailing Schedule and the Shear Modulus G_{12} of the Shell Element in SAP

Sheathing	Stud spacing, in. (mm)	MOE of members (10^6 psi)	Required G_{12} in SAP [10^4 psi (MPa)]for each edge nail spacing				
			2-in. (51 mm)	3-in. (76 mm)	4-in. (102 mm)	6-in. (152 mm)	12-in. (305 mm)
7/16 in. (11 mm) OSB	16 or 24 (406 or 610)	1.2 to 1.6	9.43 (651)	6.38 (440)	4.86 (335)	3.34 (230)	1.81 (125)

J. Archit. Eng., 2011, 17(4): 134-143

of doors in each wall; (5) gable wall missing (three-sided structure); (6) presence of roof blocking; (7) different overhang construction (ladder versus outlooker); (8) varying the anchor bolt spacing; and (9) removing anchor bolts at key locations. The standard building geometry was used for the simulated hurricane uplift and the ASCE 7-05 pressures.

Results and Discussion

Model Validation

A 4-step validation procedure, incorporating both 2D and 3D behavior, was used to ensure the accuracy of the SAP2000 modeling techniques. First, a 2D individual truss comparison was conducted against Wolfe et al. (1986) to verify the assumptions of pinned/rigid joint connectivity within the truss. Next, a 3D roof assembly (Wolfe and McCarthy 1989) verified the load sharing response of the model. Third, a 2D investigation using multiple sources (Langlois et al. 2004; Lebeda et al. 2005; Sinha and Gupta 2009) was performed to establish the validity of the shear wall behavior. Finally, the model of the index building itself was validated against a 1/3-scale prototype tested by researchers at the University of Florida (Datin and Prevatt 2007). The results of this multipart verification process showed that the SAP2000 computer model and the simplified modeling techniques adequately characterize the structural responses observed by physical testing. Details pertaining to each verification step are provided in Martin (2010).

Correlation Model for Nailing Schedule of Sheathing

One of the primary objectives was to develop a practical means to incorporate the effect of edge nailing into the SAP model. Previous researchers modeled fasteners individually using a set of "zero-length link elements" to represent each nail, and so changing the nailing schedule required the laborious revision of the model, one nail at a time. Although this may be a reasonable approach for subassembly models, (i.e. shear wall segments), it is simply not feasible for complex full-size 3D structures.

For a given load value, the shear wall deflections predicted by the NDS code (AF&PA 2005b) were compared with those predicted by SAP2000 model. The NDS tabulates G_a values for different nailing schedules, allowing the predicted deflection of a shear wall to be computed at each possible edge nailing scenario. The goal then is to match the analytical model to each of these computed deflections by iteratively changing the shear modulus, G_{12}, in SAP. When a value of G_{12} in SAP is found to give the same deflection as predicted by the NDS equation, the correlation is complete for that particular nailing schedule. The process is repeated for each possible nailing schedule, resulting in the correlations shown in Table 4. The correlated SAP model was compared with previously published experimental results, and, as shown in Martin (2010), the correlated SAP model reasonably predicted the deflection of the shear walls.

Table 4 presents the results of the correlation study relating the shear modulus for the shell element, G_{12}, to the edge nail spacing for each panel. The extent to which edge nailing affects diaphragm or shear wall stiffness is dependent on the presence of blocking. Unblocked systems, such as residential roof systems, are relatively unaffected (in-plane unit shears) by changes in the edge nailing. On the other hand, blocked systems, such as residential wall systems (assuming the typical practice of placing OSB panels vertically), do respond to changes in the nailing schedule. Therefore, this study focuses on the effect of edge nailing in the wall sheathing (i.e., not the roof sheathing). Martin (2010) offers detailed explanations of how these correlated values were determined and how the results compare with physical shear wall tests.

Uniform Uplift Pressure

In all of the analyses, vertical reactions at the hold-downs and anchor bolts were determined. Positive values represent uplift (tension), whereas negative values represent downward forces (compression). Unless otherwise noted, the edge nailing for the wall sheathing used for all output results is 6 in. (152 mm) on center.

Standard Geometry (Control Case)

Before altering the geometry, the standard index building was loaded with a uniform uplift pressure to establish a control case with which all other arrangements could be compared. As expected, the building response was symmetric. The gable walls, or end walls, show a load intensity (i.e., spike) directly beneath the peak of the roof (see Fig. 4). This results from load accumulating in the roof structure, delivered via the ridgeline to the anchor bolt directly below it (see Fig. 5). In Fig. 5, the von Mises stresses in the shell element are displayed. The von Mises stress is a convenient method of combining the stresses (normal and shear) that act in all three directions (X, Y, and Z) into a single parameter, called the equivalent stress or von Mises stress. Doing so highlights the accumulation of load at the ridge and the subsequent concentration in the gable wall directly beneath it. For the edge nailing shown (6 in.), the load is not evenly distributed by the gable wall, and a spike in load intensity is witnessed at the anchor bolt directly below the ridge.

The side walls, or eave walls, display a parabolic reaction profile (see Fig. 6). The side wall experiences the highest reactions of all locations in the building, with the maximum occurring in the middle. In this location, load originating in the roof structure is

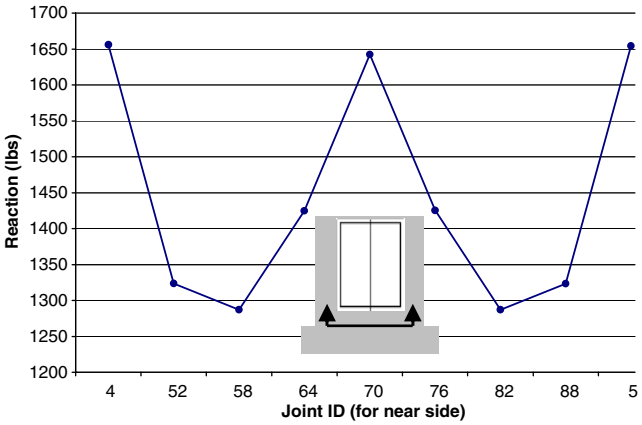

Fig. 4. Reaction profile for the gable wall, uniform uplift pressure

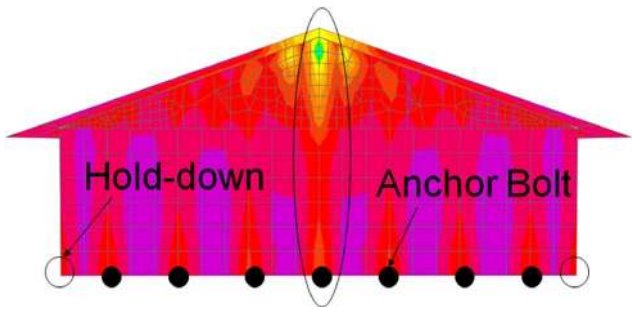

Fig. 5. Load accumulation in the gable end below the ridge of the roof

J. Archit. Eng., 2011, 17(4): 134-143

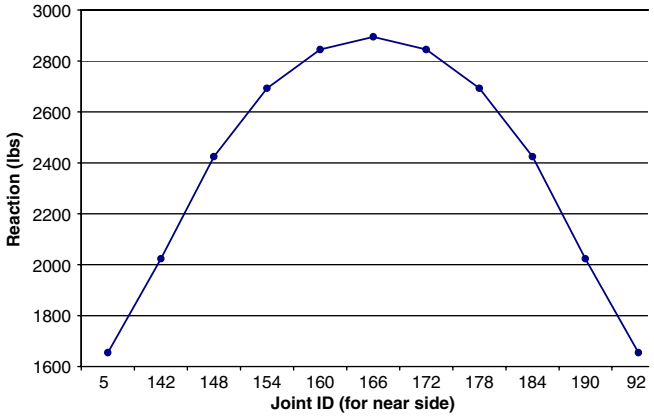

Fig. 6. Reaction profile for the side wall, uniform uplift pressure

not effectively transferred to the end walls and is, in essence, forced to the side walls. The practical implication of this finding is that an anchor bolt located in the side wall carries more load than one located in the end wall—even below the ridge line.

Effect of Edge Nailing

As the edge nailing gets denser, the wall becomes stiffer and capable of distributing the roof loads more evenly to the foundation. In looking at the 2-in. (51-mm) edge nailing reaction profile for the gable end (Fig. 7), it can be seen that the seven interior anchor bolts each carry approximately the same vertical load [about 1,400 to 1,500 lbs (6.2 to 6.7 kN)]. In comparison, the 12-in. (305-mm) nailing option produces nearly six times as much variation in anchor bolt loads [1,200 to 1,800 lbs (5.3 to 8.0 kN)] for the same uniform roof pressure. In other words, the less rigid wall is incapable of evenly distributing the roof loads, and elevated load intensities occur. A similar trend is observed in the side walls, where the more rigid 2-in. edge nailed wall more evenly distributes roof load among interior anchor bolts (Fig. 8). However, the redistribution of force in the side wall is less than the gable wall, probably because of the rigid gable end truss (acting more like a wall), which is able to transfer load more evenly to the gable walls than to side walls.

Effect of Door Openings

Door in End Wall: A 16-ft (4.9-m) opening representing a typical overhead garage door was located in the center of the end wall to examine its effect. As expected, the anchorage devices at either side of the opening carry more load (Fig. 9); however, the total uplift load carried by the gable wall is reduced by 14%, [from 12,987 lbs

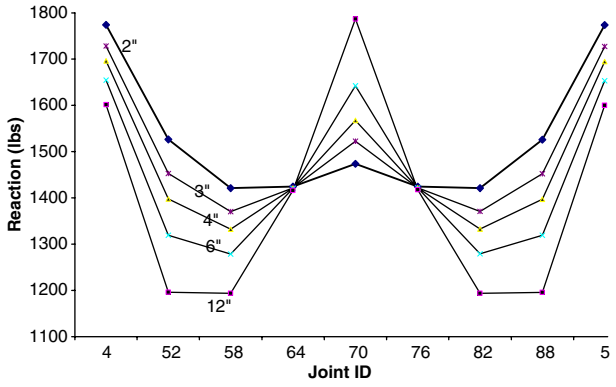

Fig. 7. Effect of edge nailing for the gable wall, uniform uplift pressure

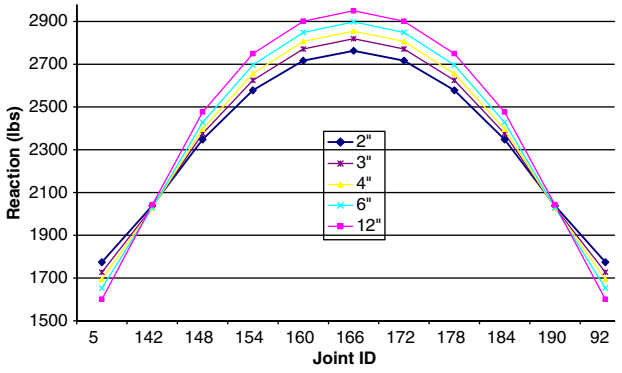

Fig. 8. Effect of edge nailing for the side wall, uniform uplift pressure

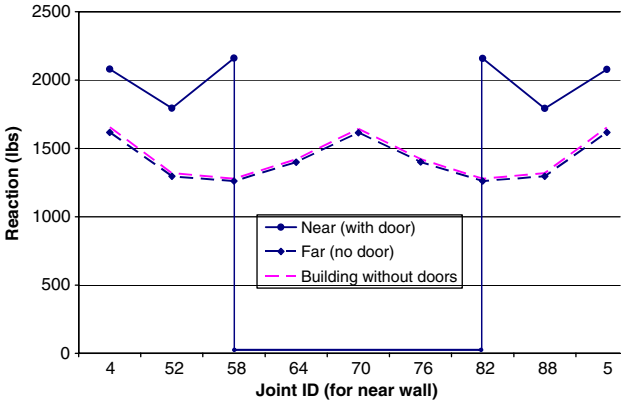

Fig. 9. Reaction profile for the end walls with a door in the center of the near side gable wall

(57.8 kN) with nine reactions to 12,063 lbs (53.7 kN) with six]. The missing 924 lbs (4.1 kN) is shed to the side wall over the first half of the building, as can be seen in Fig. 10. There is no change in the reaction profile for the opposite gable wall, the one without the door. The significance of this finding is made clear when the door is placed in the side wall instead of the end wall (see Fig. 11).

Door in Side Wall: A similar 16-ft (4.9-m) door opening was positioned in the center of the side wall, (no door in the gable end walls). In this scenario, the opening creates very large load amplifications in the reaction profile of the side wall with opening (Fig. 11). The anchor bolt reactions at the sides of the opening

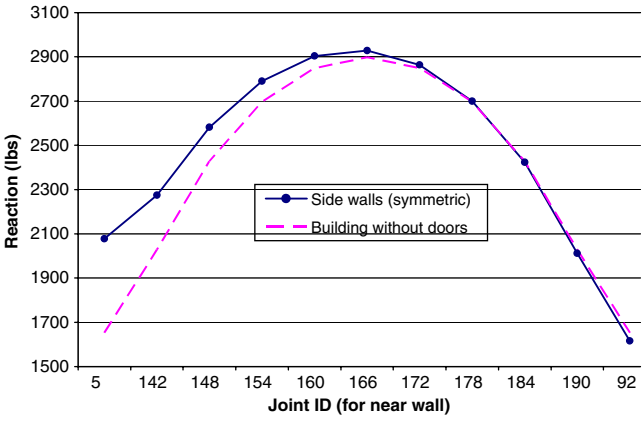

Fig. 10. Reaction profile for the side walls with a door in the center of the near side gable wall

J. Archit. Eng., 2011, 17(4): 134-143

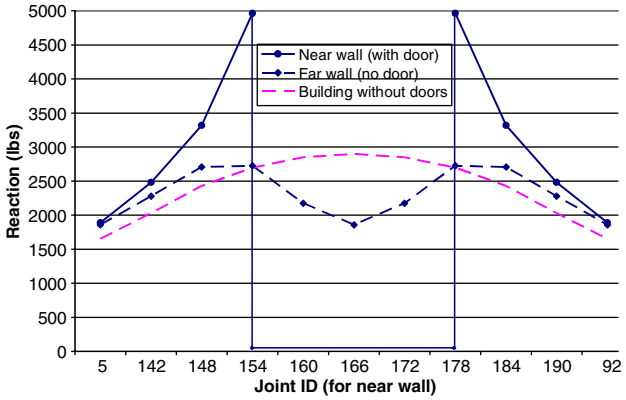

Fig. 11. Reaction profile for the side walls when a door is centered in the near side wall

nearly doubled the uplift reaction for the case of the side wall without an opening. Despite this amplification, the side wall carries reduced total load than the side wall without opening [a 908 lbs (4.0 kN) (or 29%) reduction in total vertical load]. The balance of the load is not carried by the opposite wall as might be expected, but instead it is shed evenly to the gable end walls. Further, the far side wall (Fig. 11) also carries less total load compared with the door opening present in the near side wall. This interesting system effect is attributable to the orientation of the trusses, perpendicular to the side walls. A reduction in stiffness in the front side wall (i.e., the presence of a door) produces a corresponding stiffness reduction in the far side wall. The flexibility introduced by the presence of the door affects the trusses directly atop the opening. The trusses located above or near the door opening have reduced stiffness and therefore carry less load, even though no opening is present in the far side wall. In summary, the sidewalls shed 1,778 lbs (7.9 kN) to the two gable end walls when a 16-ft (4.9-m) opening is located in one side wall. This load is shared evenly between the end walls, resulting in an 889 lbs (4.0 kN) increase in load, distributed evenly among the anchorage devices there.

The load-carrying capacity of the far side wall, the one without the door, is highly dependent on the size of the header beam used to span the door opening and the presence of a ceiling (Martin 2010). As the header depth increases, the opening becomes more rigid and thus is capable of carrying more load. However, very little of this additional load-carrying capacity is realized in the front side wall with a door opening. For example, the total front (with opening) side wall reaction only increases by 2% when the header depth is doubled [from 12 to 24 in. (305 to 610 mm)]. However, a different story unfolds on the far side wall, where the total reaction of the five anchor bolts corresponding to the door opening location, increased by about 14% [from 11,654 to 13,248 lbs (51.9 to 58.9 kN)].

A similar effect is observed when a ceiling [1/2-in. gypsum wall board (GWB) in this case] is included in the 3D structural model. The total vertical reaction capacity of this building geometry is increased, with very little change in total reaction in front side wall (with opening), and a significant increase in capacity in the far side wall (without opening) (Martin 2010). The 1/2-in. (12-mm) GWB ceiling is as effective in attracting loads to the far side wall as is the extremely deep (24-in.) header. The additional load-carrying capability comes from the increase in stiffness that the ceiling provides.

In summary, the presence of a door opening centered in the side wall always results in an increase in the load carried by the (perpendicular) gable end walls. More flexible headers cause the side walls to shed more load to the gable end walls than occurs with stiffer headers. The effect of several additional geometric scenarios studied are discussed in Martin (2010).

Simulated Hurricane Uplift Pressures

The simulated hurricane uplift pressures were determined from a wind tunnel study on a 1:50 scale model of the house (Datin and Prevatt (2007). Three hundred and eighty-six pressure taps installed on the roof provided pressure-coefficient time histories that were used to develop pressure distributions for five incident wind azimuths of 0, 45, 90, 135, and 180°. The pressure coefficients converted to full-scale pressures [normalized by a 3-s gust design wind speed of 130 mi/h (58 m/s) in open terrain exposure], for comparison with ASCE 7-05 design values. The 45° wind azimuth produced the highest pressures on the roof out of the five wind directions tested in the wind tunnel. The vertical reactions to local maxima pressures distributed over the roof (for wind azimuth 45°) are reported in the next section. The discussions on two additional load cases are provided in Martin (2010). Fig. 12 shows the reaction profile attributable to local maxima uplift pressures for wind azimuth 45°, using 6-in. (152-mm) on center edge nailing of the wall sheathing. Positive values represent uplift, for both applied pressure and observed reactions.

The reaction profiles of the gable end walls behave as expected, with the windward wall experiencing more uplift than the leeward wall. The leeward side wall experiences the highest uplift because the leeward roof area carries greater pressure. There is a significant drop in the uplift reaction in the leeward side wall (dashed line). This occurs because a net lateral force "racks" the structure toward the leeward corner of the building. The lateral forces arise because of the unbalanced horizontal component of the uplift pressures, which are oriented normal to the sloped roof surfaces.

ASCE 7-05 Pressures

Three scenarios were considered with the ASCE 7-05 pressures: (1) vertical component of uplift acting alone, (2) horizontal component of uplift pressures acting alone, and (3) a resultant uplift pressures (horizontal and vertical components). The results of scenarios 2 and 3 are provided in Martin (2010). Case 1 is discussed in this section and is compared with simulated hurricane loads, as shown in Fig. 13. The general shape of the reaction profiles is similar to that which was witnessed for the uniform pressure scenarios (Fig. 4). The magnitude of the reaction values is slightly different, though, because the applied load is not identical to the uniform pressure cases.

It is of particular importance to determine whether or not the code-based design loads (ASCE 7-05) adequately address the sustained effects from extreme wind events such as hurricanes. The current study offers a unique insight into this area of interest. The uplift reactions predicted by the SAP model are compared among the three simulated hurricane load scenarios and the ASCE 7-05 uplift-only scenario (Fig. 13). It can be seen that the current code procedure satisfactorily encompasses the foundation load results collected using the three hurricane simulations.

SAP versus Wood Frame Construction Manual

In addition to the numerous validations already noted, the results from the SAP model can also be compared with values tabulated in the *Wood Frame Construction Manual* (WFCM) published by the American Forest and Paper Association (2001). The most noteworthy comparison comes from Table 2.2A in the WFCM, wherein uplift connection loads are tabulated at different wind speeds. To make a direct comparison to SAP, no dead load is assumed to act within the building. Thus, the WFCM gives an uplift connection

J. Archit. Eng., 2011, 17(4): 134-143

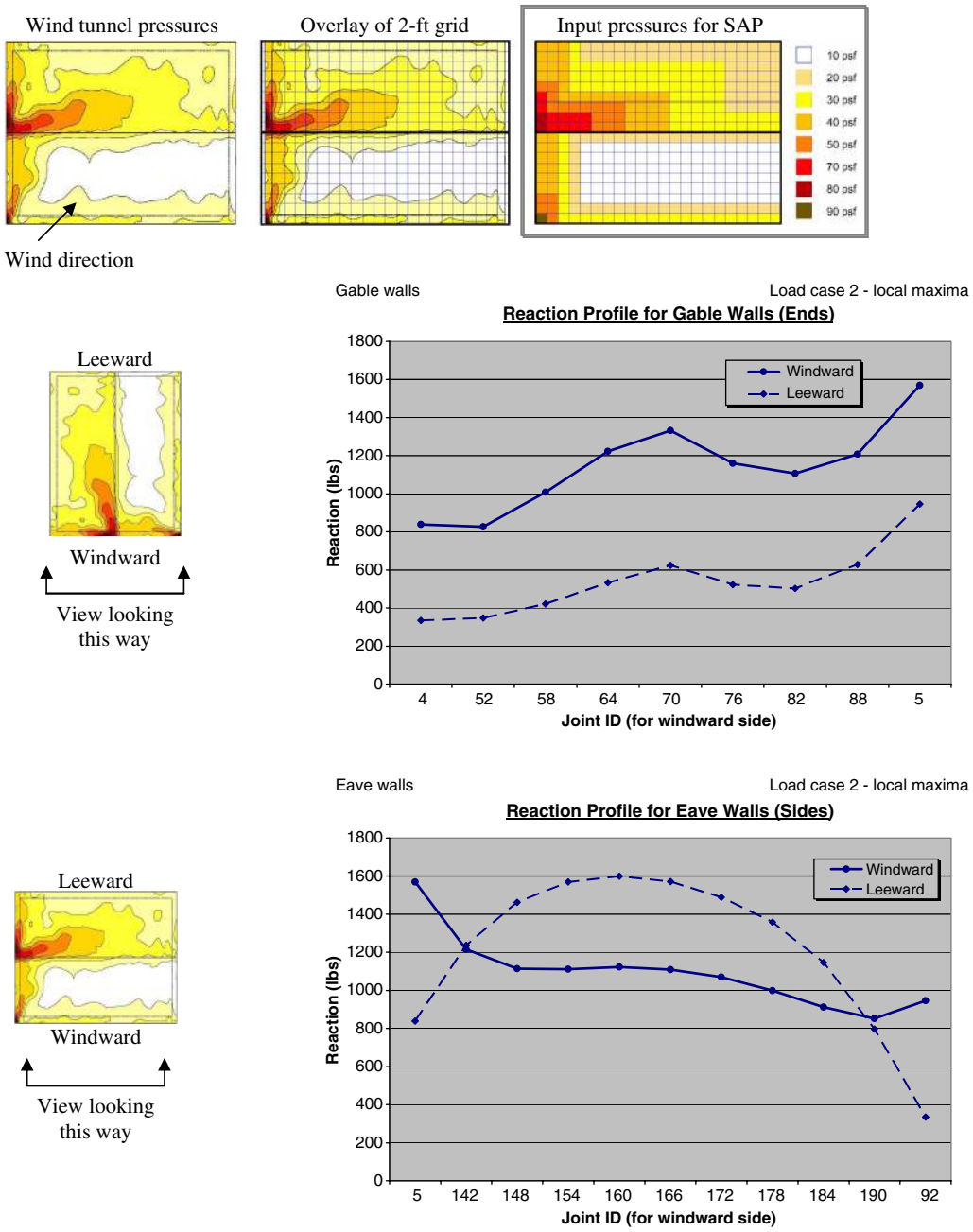

Fig. 12. Wind tunnel pressures, load case 2—local maxima over the entire roof

load of 548.5 lb/ft (8 N/mm). With anchor bolts spaced at 4-ft intervals, this translates into an individual uplift load of 2,194 lbs (9,763 N). This value is derived using the main wind force-resisting system (MWFRS) pressures given by ASCE (considering only uplift). For comparison, the maximum individual uplift reaction predicted by the SAP model is 2,244 lbs (9,986 N) (+2% difference), which is obtained by applying C&C loads to the model (Martin 2010).

Although the two values show good agreement, the most significant ramification of this comparison is that the WFCM uses MWFRS pressures to derive the tabulated values, whereas the SAP model uses C&C pressures. Martin (2010) provides a more thorough explanation of the difference between these two types of wind loads, but for the present discussion, it is important to realize that the C&C pressures represent localized peak loads acting directly on primary structural elements (i.e., roof sheathing). In contrast, MWFRS pressures were developed for secondary structural members, which do not receive wind loads directly. Therefore, MWFRS pressures are generally lower than their C&C counterparts because the localized effects that cause the higher pressure coefficients for components and cladding are effectively averaged by the time these forces make their way into the MWFRS elements (AF&PA 2001). In other words, ASCE 7-05 and the WFCM acknowledge that there are system effects at play within the structure that reduce the intensity of the wind loads as they are transmitted throughout the building. However, they have no way of accounting for these system effects directly. Instead, the code compensates by using two completely different sets of wind loads.

The advantage of using a computerized 3D structural analysis tool (e.g., SAP) is that system effects are inherently incorporated, which potentially eliminates need for two distinct design wind load provisions. The results of this study suggest this potential benefit,

J. Archit. Eng., 2011, 17(4): 134-143

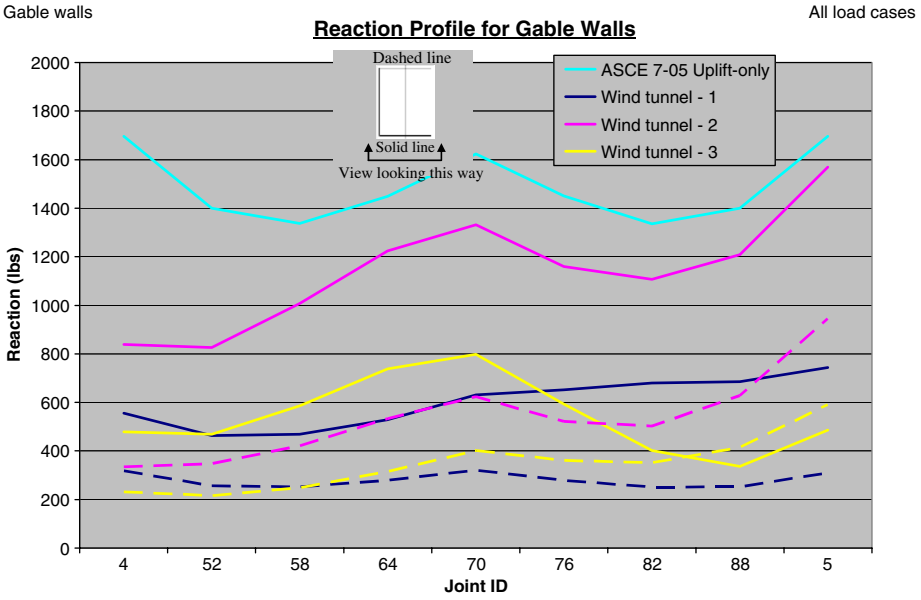

Fig. 13. Comparison between uplift reactions using ASCE 7-05 and those predicted by the simulated hurricane events; the solid line represents the windward end wall, and the dashed line signifies the opposite, leeward end

observing that despite applying component and cladding pressures to the primary structural system (i.e., sheathing), the program's output for foundation-level forces are nearly identical to (within 2% of) the forces predicted by the MWFRS design provisions. However, further study for different building geometries and load locations will be needed to determine whether this finding is universally applicable for all (or a specific class of) low-rise buildings.

Conclusions

The following conclusions are formed on the basis of research conducted in support of this project and, therefore, pertain only to the specific load cases previously described.

1. The 3D computer model and techniques developed within this research effort successfully predicted the behavior of complex, three-dimensional, wood-framed structures subjected to wind uplift pressure.
2. A novel correlation procedure and modeling technique developed simplifies modeling procedures for blocked edge wood shear walls by eliminating the need for including individual fasteners in the analytical model. Thus, a simple thick shell element with mesh-generated subelements can be used to model a complete wall or roof surface. The adjustments in nailing schedule are applied by changing a single parameter, the G_{12} bulk modulus.
3. Near the ends of the building, load accumulates at the ridgeline of the roof and is transferred to the gable walls directly below the roof peak.
4. When subjected to uniform uplift loads, anchor bolts located in the side walls experience the highest uplift reactions.
5. The wall edge nailing density strongly influences the ability of the walls to share roof-level loads.
6. The addition of a large door opening to any wall results in a loss of load carried by the entire wall.
7. The extent to which a variation in the geometry (e.g., the presence of an opening) on one side of the building affects the opposite side of the building is highly dependent on the orientation of the trusses.
8. ASCE 7-05 component and cladding pressures adequately predict the expected uplift loads from extreme wind events such as hurricanes. The uplift reactions predicted by the SAP model when loaded with the ASCE 7-05 C&C pressures (uplift only) fully encompass those of the simulated hurricane events at the same basic wind speed.
9. The analytical model developed in this study accurately predicted the MWFRS uplift forces at the foundation level when using ASCE 7-05 component and cladding pressures applied to the roof. To account for system effects, foundation-level forces are conventionally computed using the MWFRS set of wind loads from ASCE 7-05. The results suggest a single set of wind design provisions may be suitable for designing a structure using the 3D structural model of the building.

Acknowledgments

Funding provided by NSF (Award No. CMMI 0800023) and USDA Center for Wood Utilization research grant is greatly appreciated.

References

American Forest and Paper Association (AF&PA). (2001). "Wood frame construction manual." *ANSI/AF&PA WFMC-2001*, Washington, DC.

American Forest and Paper Association (AF&PA). (2005a). "National design specification for wood construction." *ANSI/AF&PA NDS-2005*, Washington, DC.

American Forest and Paper Association (AF&PA). (2005b). "Special design provisions for wind and seismic." *ANSI/AF&PA SDPWS-2005*, Washington, DC.

American Forest and Paper Association (AF&PA). (2007). "Connection design." *DES110*, Washington, DC.

ASCE. (2005). "Minimum design loads for buildings and other structures." *ASCE/SEI 7-05*, New York.

Asiz, A., Chui, C. Y., Smith, I., and Bartlett, M. (2010a). "Full-scale destructive test on wood lightframe structures." *World Conf. on Timber Engineering* (CD-ROM), CNR-IVALSA, Trees and Timber Institute, Florence, Italy.

Asiz, A., Chui, C. Y., Zhou, L., and Smith, I. (2010b). "Three-dimensional numerical model of progressive failure in wood light-frame buildings." *World Conf. on Timber Engineering* (CD-ROM), Riva del Garda, Italy.
Computers and Structures, Inc. (2008). *CSI Analysis Reference Manual: SAP2000, ETABS and SAFE*, Berkeley, CA.
Datin, P. L., and Prevatt, D. O. (2007). "Wind uplift reactions at roof-to-wall connections of wood-framed gable roof assembly." *12th Int. Wind Engineering Conf.*, Australasian Wind Engineering Society, Cairns, Australia.
Dikkers, R. D., Marshall, R. D., and Thom, H. C. S. (1970). *Hurricane Camille—August 1969: A survey of structural damage along the Mississippi Gulf Coast*, National Bureau of Standards, Washington, DC.
Doudak, G. (2005). "Field determination and modeling of load paths in wood light-frame structures." Ph.D. thesis, McGill Univ., Montreal, Quebec, Canada.
FEMA. (2006). *Hurricane Katrina in the Gulf Coast: Mitigation assessment team report—Building performance observations, recommendations, and technical guidance*, Washington, DC.
Gupta, R. (2005). "System behavior of wood truss assemblies." *Prog. Struct. Eng. Mater.*, 7(4), 183–193.
Gupta, R., and Limkatanyoo, P. (2008). "Practical approach to designing wood roof truss assemblies." *Pract. Period. Struct. Des. Constr.*, 13(3), 135–146.
Gupta, R., Miller, T. H., and Dung, D. (2004). "Practical solution to wood truss assembly design problems." *Pract. Period. Struct. Des. Constr.*, 9(1), 54–60.
Hill, K. M., Datin, P. L., and Prevatt, D. O. (2009). "Revisiting wind uplift testing of wood roof sheathing—Interpretation of static and dynamic test results." *Hurricane Hugo 20th Anniversary Symp. on Building Safer Communities—Improving Disaster Resilience*, Applied Technology Council, Redwood City, CA.
Kasal, B. (1992). "A nonlinear three-dimensional finite-element model of a light-frame structure." Ph.D. thesis, Oregon State Univ., Corvallis, OR.
LaFave, K. D., and Itani, R. Y. (1992). "Comprehensive load distribution model for wood truss roof assemblies." *Wood Fiber Sci.*, 24(1), 79–88.
Langlois, J., Gupta, R., and Miller, T. H. (2004). "Effects of reference displacement and damage accumulation in wood shear walls." *J. Struct. Eng.*, 130(3), 470–479.
Lebeda, D., Gupta, R., Rosowsky, D., and Dolan, J. D. (2005). "The effect of hold-down misplacement on the strength and stiffness of wood shear walls." *Pract. Period. Struct. Des. Constr.*, 10(2), 79–87.
Li, Z., Gupta, R., and Miller, T. H. (1998). "Practical approach to modeling of wood truss roof assemblies." *Pract. Period. Struct. Des. Constr.*, 3(3), 119–124.
Martin, K. G. (2010). "Evaluation of system effects and structural load paths in a wood-frame building." M.S. thesis, Oregon State Univ., Corvallis, OR, ⟨http://ir.library.oregonstate.edu/jspui/handle/1957/14312⟩.
McCutcheon, W. J. (1977). "Method for predicting the stiffness of wood-joist floor systems with partial composite action." *FPL-RP-289*, Forest Products Laboratory, Madison, WI.
Mtenga, P. V. (1991). "Reliability of light-frame wood roof systems." Ph.D. thesis, Univ. of Wisconsin—Madison, Madison, WI.
Percival, D. H., and Comus, Q. B. (1980). "Load distribution in a full-scale nailed-glued hip-roof system." *For. Prod. J.*, 30(11), 17–21.
Reed, T. D., Rosowsky, D. V., and Schiff, S. D. (1997). "Uplift capacity of light-frame rafter to top plate connections." *J. Archit. Eng.*, 3(4), 156–163.
Riley, M. A., and Sadek, F. (2003). *Experimental testing of roof to wall connections in wood frame houses*, National Institute of Standards and Technology, Gaithersburg, MD.
Seaders, P. (2004). "Performance of partially and fully anchored wood frame shear walls under monotonic, cyclic, and earthquake loads." M.S. thesis, Oregon State Univ., Corvallis, OR.
Seaders, P., Gupta, R., and Miller, T. H. (2009). "Monotonic and cyclic load testing of partially and fully-anchored wood-frame shear walls." *Wood Fiber Sci.*, 41(2), 145–156.
Simpson Strong-Tie Company, Inc. (2008). "Wood construction connectors." *C-2009 Product Catalog*, Pleasanton, CA.
Sinha, A., and Gupta, R. (2009). "Strain distribution in OSB and GWB in wood-frame shear walls." *J. Struct. Eng.*, 135(6), 666–675.
Sutt, E. G., Jr. (2000). "The effect of combined shear and uplift forces on roof sheathing panels." Ph.D. dissertation, Clemson Univ., Clemson, SC.
Taly, N. (2003). *Loads and load paths in buildings: Principles of structural design*, International Code Council, Inc., Washington, DC.
USDA. (1999). "Wood handbook: Wood as an engineering material." *USDA Forest Service FPL-GTR-113*, Forest Products Laboratory, Madison, WI.
van de Lindt, J. W., Graettinger, A., Gupta, R., Skaggs, T., Pryor, S., and Fridley, K. (2007). "Performance of woodframe structures during Hurricane Katrina." *J. Perform. Constr. Facil.*, 21(2), 108–116.
Wolfe, R. W., and LaBissoniere, T. (1991). "Structural performance of light-frame roof assemblies II. Conventional truss assemblies." *FPL-RP-499*, Forest Products Laboratory, Madison, WI.
Wolfe, R. W., and McCarthy, M. (1989). "Structural performance of light-frame roof assemblies: I. Truss assemblies with high truss stiffness variability." *FPL-RP-492*, Forest Products Laboratory, Madison, WI.
Wolfe, R. W., Percival, D. H., and Moody, R. C. (1986). "Strength and stiffness of light framed sloped trusses." *FPL-RP-471*, Forest Products Laboratory, Madison, WI.
Zisis, I. (2006). "Structural monitoring and wind tunnel studies of a low wooden building." M.S. thesis, Concordia Univ., Montreal, Canada.